AIAA 99-1872

A99-27849

A Stochastic Approach To Compute Subsonic Noise Using Linearized Euler's Equations*

Christophe Bailly† and Daniel Juvé‡

Laboratoire de Mécanique des Fluides et d'Acoustique
Ecole Centrale de Lyon & UMR CNRS 5509
BP 163, 69131 Ecully cédex, France.

Abstract

This paper introduces an improved version of the Stochastic Noise Generation and Radiation (SNGR) model, with an application to a subsonic jet noise. The SNGR model allows to simulate the generation and propagation of aerodynamic noise from a numerical solution of the Reynolds averaged Navier-Stokes equations using a $k-\epsilon$ closure. First a stochastic simulation of a turbulent velocity field is obtained by random Fourier modes. Then, this turbulent field is used as a source term in the Euler equations linearized around the mean flow previously calculated. This method was already applied to confined flows in 2-D and 3-D. Subsonic jet noise was also studied. However the SNGR model was applied with an axisymmetric calculation of the propagation. In this work, a full 3-D calculation of the propagation is carried out with an improved stochastic turbulent field for the case of a round subsonic jet.

1. Introduction

Direct estimation of aerodynamic noise provided by an unsteady solution of the compressible Navier-Stokes equations is still exceptional. Indeed, specific methods must be used in Computational AeroAcoustics (CAA) due to the disparity between aerodynamic and acoustic fields.[1,2] Even the use of compressible Large Eddy Simulations requires accurate numerical algorithms and large computing resources.[3]

If the direct approach is proscribed, it is necessary to have some idea of the physics of noise. For supersonic jets, it is now established that the radiation of instability waves is the most important contribution of noise when the convection velocity of large turbulent structures is supersonic. Linearized Euler Equations (LEE) govern this noise mechanism and provide supersonic jet noise predictions.[4] An hybrid approach is also proposed by Morris[5] *et al.* with the Non-Linear Disturbances Equations (NLDE).

The situation is quite different for aerodynamic noise generated by high-Reynolds number subsonic flows, where fine scale turbulence is the main source of mixing noise. In addition, many pratical challenges to reduce noise in industrial applications are of this case. Current engineering calculations mostly use Reynolds-Averaged Navier-Stokes Equations (RANSE). The most popular two-equation model is the $\bar{k}-\epsilon$ turbulence model, where $\bar{k}$ is the turbulent kinetic energy and ϵ the turbulence energy dissipation rate. Several methods were developed from Lighthill's analogy to provide statistical source representations[6–9] for jet noise. However, it is difficult to generalize these methods to complex geometries such as confined flows, spectral predictions are not always satisfactory due to the simplified description of turbulent correlations, and refraction effects are included in the source term rather than in the wave operator.

The Stochastic Noise Generation and Radiation (SNGR) model is based on the following two ideas. First the exact wave operator for acoustic perturbations is given by linearized Euler's equations. Secondly, since many engineering CFD methods use RANSE solutions, the SNGR model must rely on

†Assistant Professor, Member AIAA

‡Professor, Member AIAA

a $\bar{k} - \epsilon$ turbulence model. The challenge of this approach is to derive a turbulent velocity field from the knowledge of the local mean flow, which could be used as a source term in linearized Euler's equations. In the SNGR model, the turbulent velocity field is synthesized from a sum of random Fourier modes. A first formulation of this model was applied to subsonic jet noise calculation.[10,11] However the computation of the propagation was axisymmetric, with the result that the sources were completely correlated in the azimuthal direction. Applications of the model to the prediction of noise radiation in an obstructed diaphragm were also performed in 2-D[12] and more recently in 3-D.[13]

Figure 1 shows some strategies to go from CFD to CAA. In general, computational cost and required memory are inversely proportional to the number of assumptions used in models. In other words, you do not get what you do not pay for.

In this study, an improved version of the SNGR model is presented and a full 3-D calculation of propagation is carried out for a subsonic jet. The paper is organised as follows. In section 2, the formulation of the SNGR model is introduced. Next the stochastic simulation of a turbulent velocity field is explained in section 3. The numerical method for solving LEE is described in section 4, and a refraction calculation is shown as validation. Then the SNGR model is applied to a subsonic jet and results are presented in section 5. Finally, concluding remarks are given in section 6.

2. Formulation of the SNGR model

The SNGR model relies on linearized Euler equations which govern acoustic perturbations. Since high-Reynolds flows are investigated, the viscous stress tensor is negligible in this problem and Navier-Stokes equations are not relevant. The linearization is done around a known stationary mean flow (ρ_o, $\mathbf{u}_o$, p_o), where ρ, $\mathbf{u}$ and p are the density, the velocity and the pressure, respectively. The subscript o indicates the mean value of the variable. The three-dimensional linearized Euler equations may be written in the conservative form :

$$\frac{\partial \mathbf{U}}{\partial t} + \frac{\partial \mathbf{E}}{\partial x_1} + \frac{\partial \mathbf{F}}{\partial x_2} + \frac{\partial \mathbf{G}}{\partial x_3} + \mathbf{H} = \mathbf{S} \qquad (1)$$

where the unknown vector $\mathbf{U}$ is given by:

$$\mathbf{U} = [\rho', \rho_o u_1', \rho_o u_2', \rho_o u_3', p']^T ,$$

and $\mathbf{E}$, $\mathbf{F}$, $\mathbf{G}$ are the flux vectors. The vector $\mathbf{H}$ contains the refraction terms, and so, it is equal to zero for an uniform mean flow. Next a turbulent source term $\mathbf{S}$ is introduced into the equations. This term must be defined so that the wave equation corresponding to system (1) is equivalent to Lilley's equation for a sheared mean flow. Two assumptions are used in this acoustic analogy. First the turbulent field is incompressible and second, only the first order interactions between aerodynamics and acoustics are retained. Scattering of sound by turbulence is negligible for instance. Finally, the source term $\mathbf{S}$ is written as:

$$\mathbf{S} = [0, \rho_o S_1, \rho_o S_2, \rho_o S_3, 0]^T$$

with

$$S_i = -u_{tj} \frac{\partial u_{ti}}{\partial x_j} + \overline{u_{tj} \frac{\partial u_{ti}}{\partial x_j}} \qquad (2)$$

where the subscript t designates the turbulent velocity field. In other words, the expression of the source term is found as the main non-linear turbulent term when the velocity is split into a mean part, a turbulent part and an acoustic part $\mathbf{u} = \mathbf{u}_o + \mathbf{u}_t + \mathbf{u}'$ in Euler's equations. Terms involving interactions between acoustics and the mean flow are put together on the left hand side to form a wave equation. Finally, the Stochastic Noise Generation and Radiation model requires the three following steps:

(i) First, the mean flow field is calculated by solving the Reynolds averaged Navier-Stokes equations with a $\bar{k} - \epsilon$ turbulence model.

(ii) Second, a space-time turbulent velocity field $\mathbf{u}_t$ is generated from the local values of the mean flow, the turbulent kinetic $\bar{k}$ and the dissipation ϵ.

(iii) Third, linearized Euler equations (1) are solved. On the left hand side the mean flow field is used as the coefficients of the four first-order differential equations, and on the other side, the source term $\mathbf{S}$ is calculated from the synthesized turbulent field obtained in step (ii).

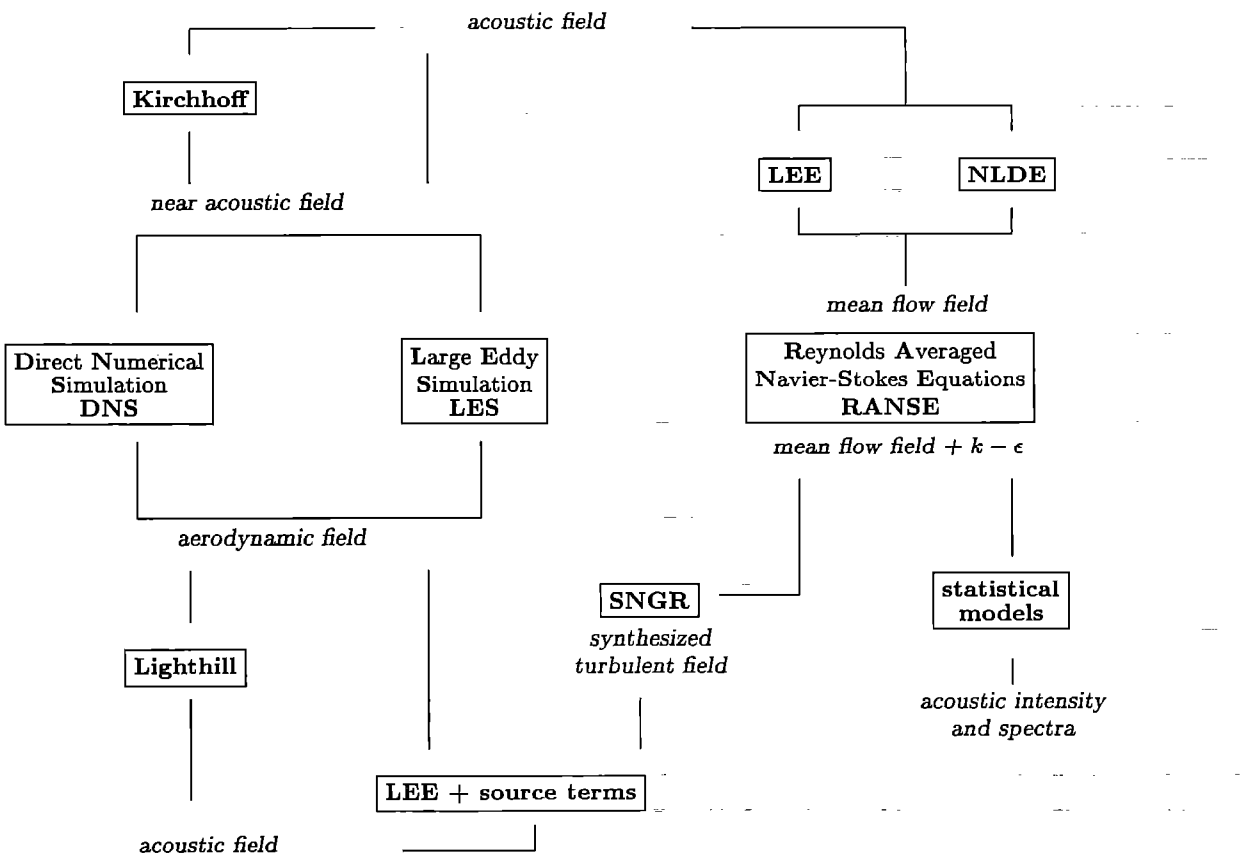

Figure 1: Some strategies to go from Computational Fluid Dynamics (CFD) to Computational AeroAcoustics (CAA). LEE means Linearized Euler's Equations, NLDE means Non Linear Disturbance Equations and SNGR means Stochastic Noise Generation and Radiation. From the chosen CFD method, acoustics is obtained from a compressible unsteady solution in the upper part whereas an acoustic analogy is used in the lower part of the diagram.

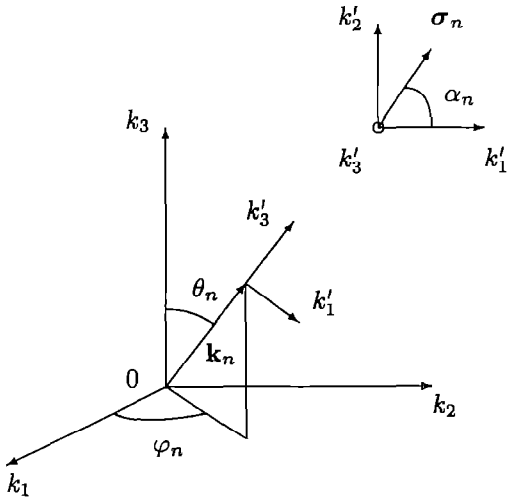

Figure 2: Sketch of the geometry for the nth Fourier random mode. The isotropic 3-D field requires the following probability density functions for the random variables φ_n, and θ_n: $p(\varphi) = 1/\pi$ and $p(\theta) = 1/2 \sin\theta$ with $0 \leq \varphi \leq \pi$ and $0 \leq \theta \leq \pi$. The unit vector $\boldsymbol{\sigma}_n$ carrying the Fourier contribution is perpendicular to the wave vector $\mathbf{k}_n$ and its polar angle α_n has an arbitrary orientation: $p(\alpha) = 1/(2\pi)$ with $0 \leq \alpha \leq 2\pi$.

For step (ii), the turbulent velocity fluctuations could be provided by a simulation of Navier-Stokes equations, by a large eddy simulation for instance.[14] In the present study, one assumes that only a numerical solution of RANSE is known. So, a space-time velocity field must be synthesized at each point of the source volume in using the knowledge of the turbulent mean flow. The next section is devoted to the generation of this stochastic turbulent field.

3. Stochastic simulation of a turbulent velocity field

Following Kraichnan[15] and Karweit[16] *et al.* a spatial stochastic turbulent velocity field is generated as a finite sum of N statistically independent random Fourier modes:

$$\mathbf{u}_t(\mathbf{x}) = 2\sum_{n=1}^{N} \tilde{u}_n \cos(\mathbf{k}_n.\mathbf{x} + \psi_n)\,\boldsymbol{\sigma}_n \qquad (3)$$

where $\tilde{u}_n$, ψ_n and $\boldsymbol{\sigma}_n$ are the amplitude, the phase and the direction of the nth mode. Figure 2 displays a sketch of the geometry. The wave vector $\mathbf{k}_n$ is picked randomly on a sphere of radius k_n to ensure isotropy. Incompressibity of the turbulent field involves $\mathbf{k}_n.\boldsymbol{\sigma}_n = 0$ for each mode n. The phase ψ_n is chosen with uniform probability to obtain an homogeneous field. The Reynolds stress anisotropy tensor:

$$b_{ij} = \frac{\overline{u_{ti}u_{tj}}}{2\bar{k}} - \frac{1}{3}\delta_{ij}$$

which describes the deviation from isotropy, is free from the random field (3). By the central limit theorem, the velocity field is normal, and so, the skewness factor is zero and the Kurtosis factor is equal to 3.

The amplitude $\tilde{u}_n$ of each mode is determined from the turbulent kinetic energy spectrum E. Since the N modes are statistically independent, the turbulent kinetic energy is given by:

$$\bar{k} = \sum_{n=1}^{N} \tilde{u}_n^2 \qquad \text{and so,} \qquad \tilde{u}_n = \sqrt{E(k_n)\,\Delta k_n}$$

A logarithm distribution of the N modes usually provides a better discretization of the spectrum E in the lower wave number range corresponding to the larger energy containing eddies:

$$k_n = \exp\left[\ln k_1 + (n-1)\,dk_l\right]$$

for $n = 1, \ldots, N$, where $dk_l = (k_N - k_1)/(N-1)$. A von Kármán - Pao spectrum is used to simulate the complete spectrum:

$$E(k) = \alpha \frac{u'^2}{k_e} \frac{(k/k_e)^4}{\left[1 + (k/k_e)^2\right]^{17/6}} \exp\left[-2\left(\frac{k}{k_\eta}\right)^2\right] \qquad (4)$$

where k is the wave number, $k_\eta = \epsilon^{1/4}\nu^{-3/4}$ is the Kolmogorov wave number, corresponding to the smallest turbulent structures ensuring viscous dissipation, ν is the molecular viscosity and u' is the r.m.s. value of the velocity fluctuations connected to the turbulent kinetic energy by $u'^2 = 2\bar{k}/3$. The two Kármán-Howarth functions f and g calculated from velocity field correlations match well with those calculated from the expression (4) of the turbulent energy spectrum.[16,11]

The spectrum $E(k)$ is normalized by the following integral relation:

$$\bar{k} = \int_0^\infty E(k)\,dk \qquad (5)$$

Then the numerical constant in expression (4) is given by:

$$\alpha = \frac{55}{9\sqrt{\pi}} \frac{\Gamma\left(\frac{5}{6}\right)}{\Gamma\left(\frac{1}{3}\right)} \simeq 1.453$$

The dissipation rate may be estimated from the energy of the large eddies u'^2 and their time scale L/u', that is $\epsilon \simeq u'^3/L$. The integral length scale L is calculated with the longitudinal one-dimensional spectrum:

$$E_{11}(k_1) = \frac{1}{2} \int_{k_1}^{\infty} \frac{E(k)}{k} \left(1 - \frac{k_1^2}{k^2}\right) dk$$

Thus, the wave number k_e associated with the most energetic eddies corresponds to the maximum of the spectrum E, which reaches its maximum in $\sqrt{12/5}\, k_e$, is calculated with the following relation:

$$L = \frac{\pi}{u'^2} E_{11}(k_1 = 0) = \sqrt{\pi} \frac{\Gamma\left(\frac{5}{6}\right)}{\Gamma\left(\frac{1}{3}\right)} \frac{1}{k_e} \qquad (6)$$

Another similar relationship can be obtained from the integral definition of ϵ, and it is in agreement with (6). Details are given in Appendix A. In all the previous expressions, we assume the turbulent kinetic energy $\bar{k}$ and the dissipation rate ϵ are known from the RANSE solution.

Time dependence must be introduced in expression (3) to get suitable statistical properties. Thus, the turbulent velocity $\mathbf{u}_t(\mathbf{x}, t)$ is now generated by a sum of unsteady random Fourier modes:

$$\mathbf{u}_t(\mathbf{x}, t) = \qquad (7)$$
$$2 \sum_{n=1}^{N} \tilde{u}_n \cos\left[\mathbf{k}_n . (\mathbf{x} - t\mathbf{u}_c) + \psi_n + \omega_n t\right] \boldsymbol{\sigma}_n$$

where $\mathbf{u}_c$ is the convection velocity and ω_n is the angular frequency associated to the nth mode. The convection velocity is a function of the known local mean flow whereas ω_n is a random variable. A simple convected field is obtained when all the ω_n are taken as zero. In Kraichnan's formulation,[15,17] ω_n and k_n are independent, which is not satisfactory for aerodynamic noise generation. In order to keep the problem as simple as possible, a Gaussian probability density function is chosen for ω:

$$p_n(\omega) = \frac{1}{\omega_{on}\sqrt{2\pi}} \exp\left(-\frac{(\omega - \omega_{on})^2}{2\omega_{on}^2}\right) \qquad (8)$$

where the mean angular frequency of the nth mode $\omega_{on} = u' k_n$ is a function of the wave number.[18] Unlike previous studies,[11,8,13] the eddy circulation time corresponding to the Heisenberg time $\tau_H \sim (u'k)^{-1}$ is used as the spectrally local characteristic time.

The source volume where the velocity field must be synthesized is limited to the initial mixing layer and the transition region for a jet. This volume is identified by comparison with the turbulent kinetic energy field. A space-time realization of the stochastic field is obtained over this volume with a drawing of the random variables for each mode. Turbulence is locally isotropic, and inhomogeneous over the whole volume. In fact, the two parameters k_e and ω_{on} vary with position $\mathbf{x}$. In this way, the integral length scale of turbulence increases continuously in the downstream direction. A defect of the inhomogeneous property is that the velocity field is not exactly solenoidal by forcing $\mathbf{k}_n . \boldsymbol{\sigma}_n = 0$, but the difference is small if the meanflow field is slowly variable. In this study, the turbulent source volume is not split into several subdomains, corresponding to independant acoustic sources.[11,8,13]

4. Numerical procedure and validation

The numerical algorithm for integrating linearized Euler's equations (1) is briefly described in this section. The computed solution is obtained by using the Dispersion Relation Preserving scheme of Tam & Webb[19] in space, combined with a fourth-order Runge-Kutta algorithm in time.[20] For boundary treatement, the nonreflecting radiation and boundary conditions of Tam & Webb[19] are implemented. For the outflow boundary, Tam & Webb's formulation is used and a perfectly matched layer[21] (PML) is applied when instability waves convected by the meanflow field are too strong. In order to validate the numerical method, radiation of multipolar sources and propagation in a sheared mean flow was investigated in 2-D geometry.[22,23] A 3-D refraction calculation is proposed as validation of the algorithm.

All the variables are made dimensionless using the following scales: Δ for the length scale, c_∞ for the velocity scale, Δ/c_∞ for the time scale, ρ_∞ for the density scale and $\rho_\infty c_\infty^2$ for the pressure scale, where Δ is the smallest mesh step size and c_∞ the ambient speed of sound.

The sheared mean flow is modelled by the following Bickley profile:

$$u_o = \frac{0.5}{\cosh^2\left[(1+\sqrt{2})\, r_\perp / b\right]} \qquad (9)$$

where the half-width b of the jet is taken as $b = 10$ and $r_\perp$ is the radial coordinate $r_\perp = \sqrt{x_2^2 + x_3^2}$. This reference test case was already studied in 2-D.[22] A regular mesh of 107^3 points is used, and a monopole source is placed on the jet axis at $x_1 = 25$ and $x_2 = x_3 = 0$. The source term $\mathbf{S}$ in the system (1) takes the form:

$$\mathbf{S} = \epsilon \, \sin \omega t \, e^{-\alpha\left(x_1^2 + x_2^2 + x_3^2\right)} \times [1, 0, 0, 0, 1]^T \qquad (10)$$

with $\alpha = \ln 2/9$. The amplitude is taken as $\epsilon = 0.01$ and the angular frequency is $\omega = 2\pi/9$, corresponding to a high frequency radiation since the Strouhal number based on the jet diameter $D = 2b$ and the velocity $u_o = 0.5$ is St $= 4.4$. The wavelength of the source is of the same order of magnitude as the half-width of the jet producing refraction effects. Figure 3 shows a snapshot of the pressure field. Wave fronts generated by the source are strongly modified by the mean flow gradients. The acoustic intensity reaches a peak in the downstream direction near the angle θ given by the relation $\cos\theta = 1/(1+M)$. For smaller angles, the intensity decreases and a shadow zone is observed. The calculated solution favorably compare with ray tracing, as shown in Figure 4.

The code has been vectorized up to 520 MFlops on a Cray C90 with 1.2 million grid points in this case, given a time per iteration and per node of 1.9μs. By comparison, the same calculation on a Dec α at 625 MHz is 30 times longer.

5. Subsonic jet noise simulation

The SNGR model is now applied to subsonic jet noise. The geometry is based on the experimental configuration of Lush,[24] for a $M = 0.86$ subsonic jet with a nozzle diameter of $D = 25 \times 10^{-3}$ m. The meanflow field was calculated in a previous study[9] with a $\bar{k} - \epsilon$ turbulence model. Good agreement was obtained with the experimental data for the mean axial velocity, the self-similar radial profiles of the velocity and the turbulence intensity. The RANSE solution is then interpolated on the acoustic computational domain.

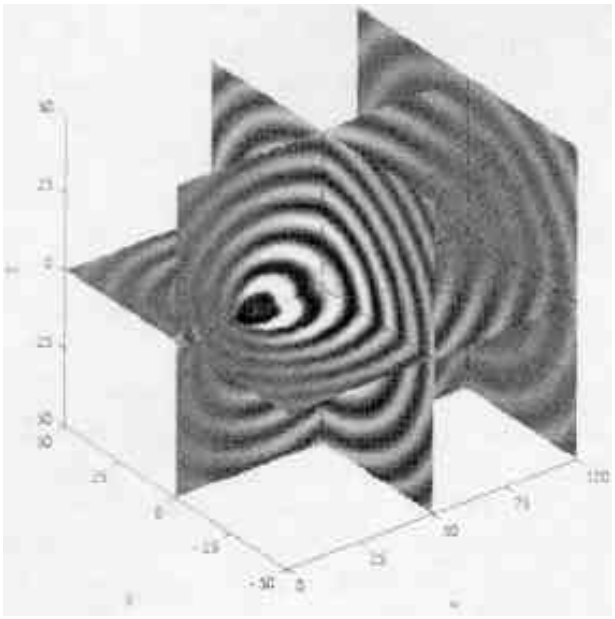

Figure 3: Snapshot of the pressure field radiated by a monopole source located in the jet profile (9) at dimensionless time $t = 225\Delta t = 135$. Pressure levels from -2×10^{-3} to 2×10^{-3}. Notations: $x_1 = x$, $x_2 = y$ and $x_3 = z$.

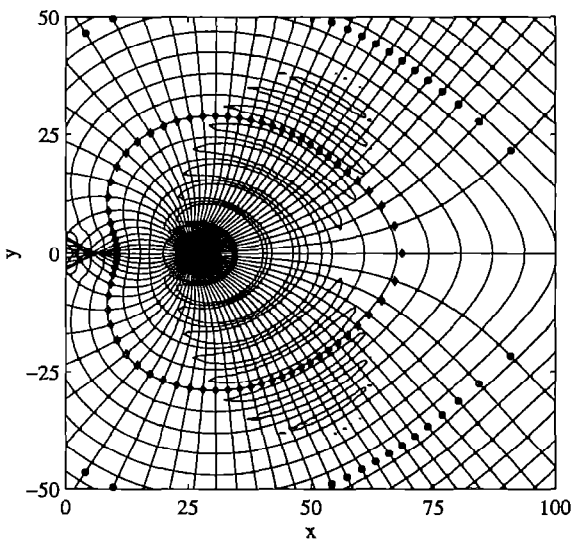

Figure 4: Pressure iso-contours in the $x_1 - x_2$ plane and comparison with a ray-tracing: 36 rays are plotted from 0 to π, and two wave fronts are marked by symbols. Notations: $x_1 = x$ and $x_2 = y$.

A preliminary calculation of a monopole source radiation is performed using the source definition (10) with $\omega = 2\pi/20$, and $x_s = 3D$. For this test case, propagation is computed over a stretched mesh of 107^3 points, with $\Delta x_1 = \Delta x_2 = \Delta x_3 = D/30$ at the nozzle exit. The meanflow field is provided by the RANSE solution and is interpolated on the acoustic grid. Figure 5 shows the instantaneous pressure field. Refraction effects are more marked than in the calculation studied in the test case of section 4, due to higher meanflow gradients.

For the SNGR model, the acoustic grid is defined as follows. In the x_2 and x_3 directions, the mesh is stretched from the jet axis, with an initial grid spacing $\Delta = 10^{-3}$ m, and so $D/\Delta = 25$. In the downstream direction, the initial grid spacing is taken as $\Delta x_1 = 2\Delta$. The irregular mesh has $137 \times 127 \times 127$ points in the $x_1 \times x_2 \times x_3$ directions corresponding to a physical domain displayed in Figure 6. The computation of propagation with the SNGR model requires in this case a memory size of 103 megawords, with a CPU speed of 470 MFlops for 2.2 million grid points.

The turbulent source volume is defined as the set of points where the turbulent kinetic energy is greater than $0.3 \times \bar{k}_{max}$, and where the integral length scale $L \simeq u'^3/\epsilon$ has at least 6 mesh points because of numerical requirements. A realization of the stochastic field is then carried out with the unsteady random Fourier mode method (8). Only the random variables and vectors of the N modes are stored for each point of the source volume, rather than the complete turbulent field for all the grid points and with each time step of the calculation. The synthesized field is generated with the following parameters: $N = 30$ modes, $k_N = 2\pi/(7\Delta x_1)$ and $k_1 = k_{emin}/5$ where k_{emin} is the smallest value of k_e over the source volume. In this way, the mesh supports propagation of acoustic signals up to $\mathrm{St} = D/(7\sqrt[3]{2})/M \simeq 3.3$ in term of Strouhal number $\mathrm{St} = (D/\lambda)/M$ with M=0.86 and a reference step size of $\Delta r = \sqrt[3]{\Delta x_1 \Delta x_2 \Delta x_3} = \sqrt[3]{2}\Delta$. A realization of the stochastic turbulent field is plotted in Figure 7. The source volume is located near the end of the potentiel core, and contains 82389 mesh points in 3-D. Several space modes can be observed, and the associated wavelengths increase in the downstream direction. The source volume is weighted by a window in order to cancel turbulent fluctuations on their boundaries.

Figure 8 shows a snapshot of the pressure field over the whole computational domain at the last time step $t = 1080\Delta t = 522.86$. Instability waves are generated by the sources, and are then convected by the mean flow in the downstream direction. An acoustic radiation is observed outside the mean flow. Axial pressure profiles are plotted in Figure 9 to show instabilities are neutralized by the PML. In order to estimate aerodynamic pressure fluctuations, radial profiles are also plotted in Figure 10 at different time intervals.

The calculated pressure is recorded along the line $x_2/D = x_3/D = 4.51$ to evaluate the acoustic directivity and the spectral content. This numerical antenna is not in the acoustic and geometric far field according to usual criteria. The Sound Pressure Level is calculated as:

$$L_p(\mathbf{x}) = L_p(r,\theta) = 10\log_{10}\left(\frac{\overline{\tilde{p}'^2}}{p_{ref}^2}\right)$$

where $\tilde{p}' = \rho_\infty c_\infty^2 p'$ is the dimension pressure fluctuation and $p_{ref} = 2 \times 10^{-5}$ Pa. The time average computation is performed over a time $T = 600\Delta t$ corresponding to signals recorded after a transitional period. The SPL is then calculated in taking into account the variation of the observation distance with respect to the nozzle exit, assuming a $1/r^2$ dependence. The acoustic intensity is also corrected by the square of the ratio $r/(120D)$ in order to compare with Lush[24] experimental data. For an observation angle $\theta = 90°$ and $r = 120D$, the present calculation gives an SPL of 80 dB whereas measurements provide 93 dB.

This first application of the SNGR model to a 3-D subsonic jet underestimates experimental data. A weakness of the present study is the function w used to weight the source term:

$$w(\mathbf{x}) = 1 - \left(\frac{\bar{k}_{max} - \bar{k}}{\bar{k}_{max} - 0.3\bar{k}_{max}}\right)^2$$

where $0.3\bar{k}_{max} \leq \bar{k} \leq \bar{k}_{max}$. The adjustement of this function has not been studied, and the global level of turbulent kinetic energy is not conserved. This result is illustrated in Figure 12 with the radial plots of the initial and weighted turbulent velocity. In further works, it would be necessary to restore the turbulence level and to investigate spectral content of acoustic signals.

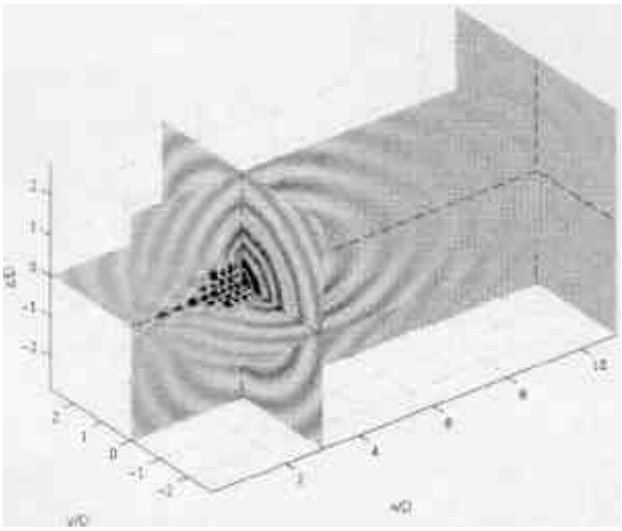

Figure 5: Radiation of a monopole source in a mean-flow field provided by a RANSE solution. Subsonic round jet at $M = 0.86$. Notations: $x_1 = x$, $x_2 = y$ and $x_3 = z$.

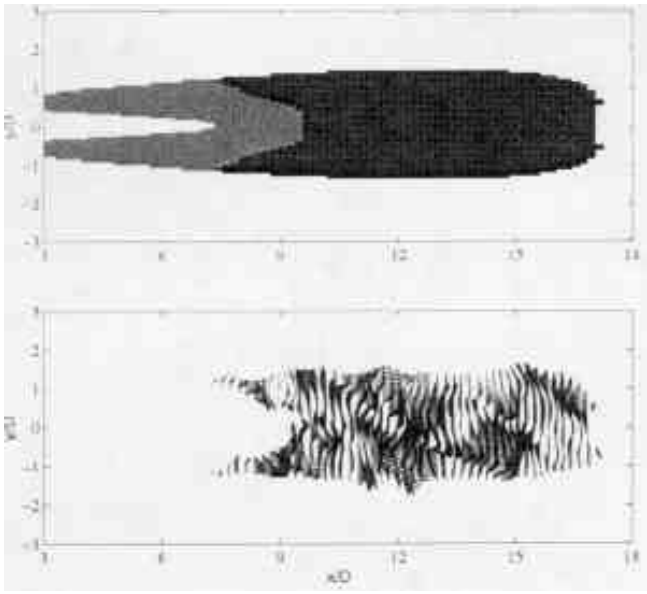

Figure 7: Zoom on the source volume in the plane $x_1 - x_2$. The upper part shows the set of points where the turbulent kinetic energy is greater than $0.3 \times \bar{k}_{max}$ in gray, and the set of points where the integral length scale is greater than 6Δ in black. The lower part shows the projection of the synthesized turbulent field at a given time on the plane $x_1 - x_2$. Notations: $x_1 = x$ and $x_2 = y$.

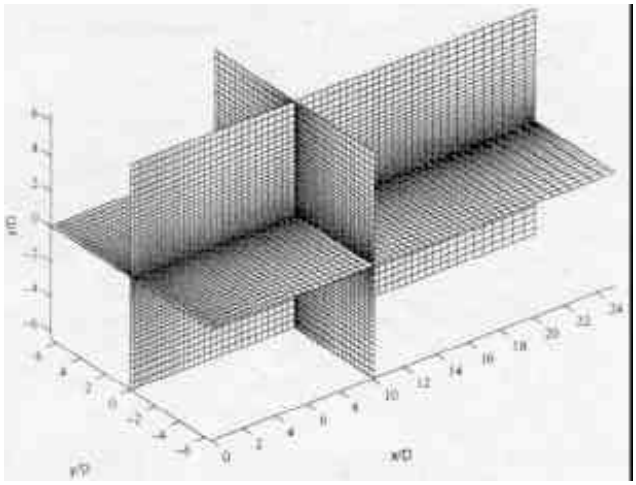

Figure 6: Computation domain for the subsonic jet noise calculation: only every second line is shown in the three directions, with $x_1 = x$, $x_2 = y$ and $x_3 = z$.

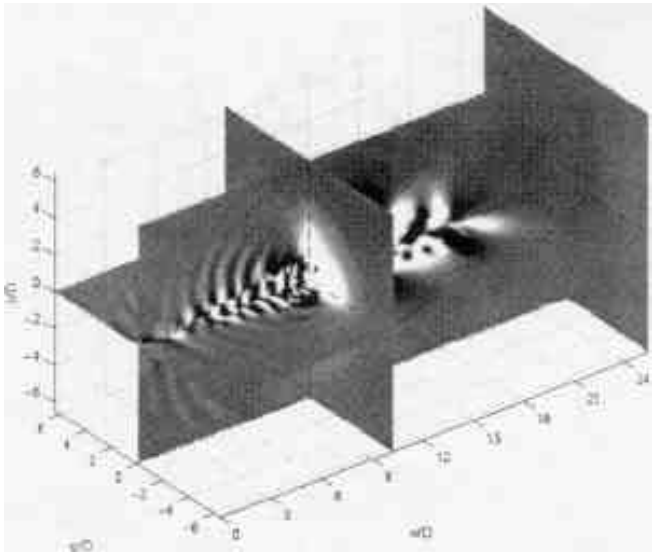

Figure 8: Calculated pressure field on the whole computational domain at time $t = 1080\Delta t = 522.86$. Pressure levels from -5×10^{-4} to 5×10^{-4}. Notations: $x_1 = x$, $x_2 = y$ and $x_3 = z$.

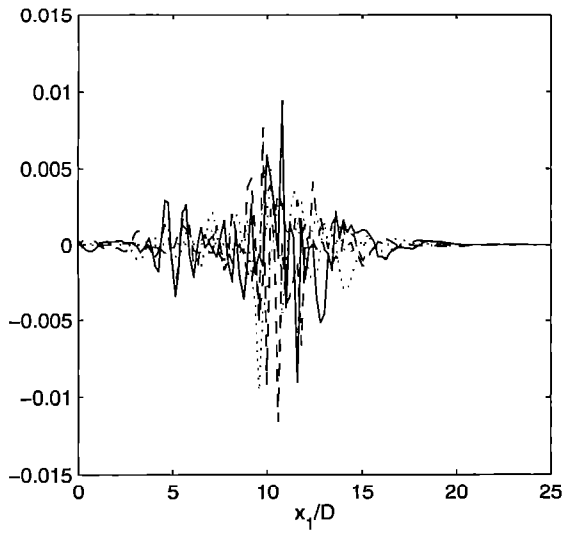

Figure 9: Pressure profiles along the jet axis. Instability waves are convected by the mean flow in the downstream direction, but their growth is saturated by the PML. Pressure fluctuations are made dimensionless by $\rho_\infty c_\infty^2$ and are not corrected by the distance.

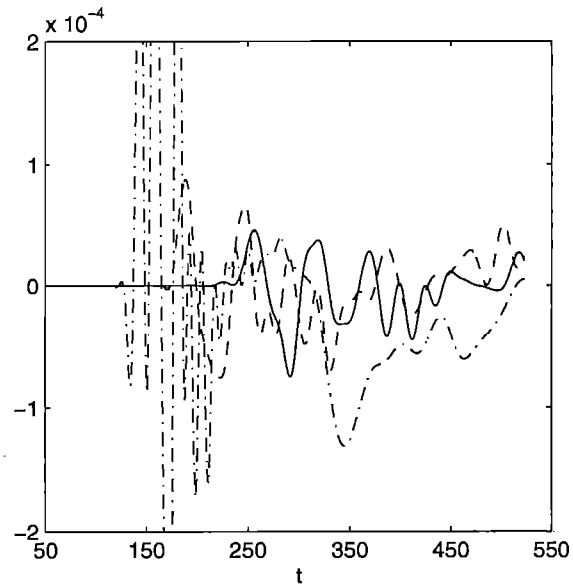

Figure 11: Pressure signals recorded in $x_2/D = x_3/D = 4.51$. —— $\theta = 90°$, ----- $\theta = 60°$, — - — $\theta = 30°$. Pressure fluctuations are made dimensionless by $\rho_\infty c_\infty^2$ and are not corrected by the distance.

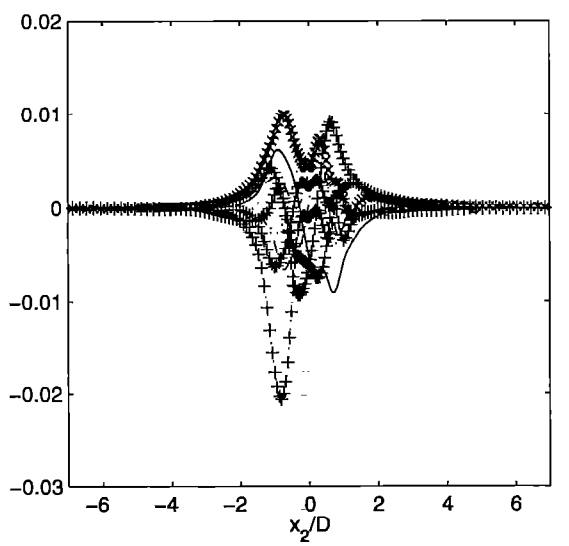

Figure 10: Pressure profiles along the x_2 axis with $x_1/D = 10.2$ (middle of the computational domain in terms of grid points), $x_3/D = 0$, and for different times. The aerodynamic pressure fluctuations are made dimensionless by $\rho_\infty c_\infty^2$.

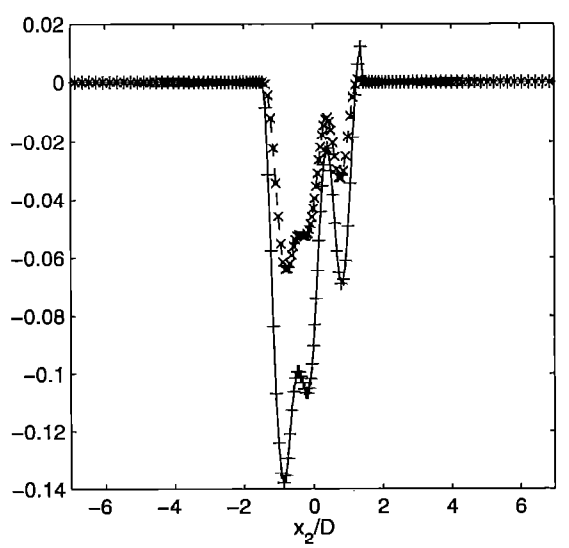

Figure 12: Radial profile of one component of the turbulent field at a given time: + expression (8), × weighing with w.

6. Concluding remarks

In this work, a new application of the Stochastic Noise Generation and Radiation model to a 3-D subsonic jet is investigated. From a numerical solution of RANSE, the SNGR model provides a stochastic turbulent field generated by a sum of unsteady random Fourier modes. This synthesized turbulent field is then used as a source term in Euler's equations linearized around the meanflow field. Generation of the stochastic field has been modified by introducing a slow space evolution of turbulence statistical properties and a spectrally local characteristic time based on Heisenberg's relation.

A jet mean flow refraction problem has been solved in 3-D. The radiation pattern is compared with a ray-tracing in order to validate the numerical algorithm. Next a similar calculation is performed, but the mean flowfield used by linearized Euler's equations is provided by a turbulence $\bar{k} - \epsilon$ model.

Finally, the 3-D SNGR model is applied to a round subsonic jet at $M = 0.86$. Turbulent source terms are generated and introduced in the LEE. First results are promising and numerical applications are under development.

Acknowledgments

The authors wish to acknowledge support of Institut du Développement et des Ressources en Informatique Scientifique (IDRIS - CNRS). This research has been conducted in cooperation with Electricité de France, Direction des Etudes et Recherches (technical monitor: P. Lafon).

Appendix A : Isotropic turbulence

The von Kármán spectrum[25] modified by Pao[26] allows the description on the complete spectral range of turbulence. From expression (4) of the turbulent kinetic energy, we can derive the following useful relations. First, the spectrum E is normalized by the relation (5) which provides the numerical constant α. Second, the energy spectrum is also normalized by the following relation:

$$\epsilon = 2\nu \int_0^\infty k^2 E(k)\, dk$$

Hence the wavevector k_e in (4) is given by:

$$\frac{u'^3}{\epsilon} = \frac{2}{k_e}\left[\alpha\Gamma\left(\frac{2}{3}\right)\right]^{-3/2} \simeq 0.725\,\frac{1}{k_e}$$

when $k_e/k_\eta \to 0$. This result is in agreement with expression (6) which provides $L \approx 0.747/k_e$ for the longitudinal integral length scale.

The simulated longitudinal correlation function:

$$u'^2 f(\mathbf{r}) = \overline{u_{ti}(\mathbf{x})\, u_{ti}(\mathbf{x}+\mathbf{r})}$$

can be compared[16,11] to those derived from the expression of the energy spectrum E:

$$f(r) = \frac{2}{u'^2}\int_0^\infty \left(\frac{\sin(kr)}{k^3r^3} - \frac{\cos(kr)}{k^2r^2}\right) E(k)\, dk$$

There are similar expressions for the transversal correlation function g. Finally, the space-time correlation function corresponding to the turbulent field generated by unsteady random Fourier modes (8) takes the form:

$$\begin{aligned} R_{\alpha\alpha}(\mathbf{r},\tau) &= 2\sum_{n=1}^{N}\left\{\sigma_{\alpha n}^2 \exp\left(-\frac{\tau^2\omega_{on}^2}{2}\right)\right. \\ &\times \left.\cos\left[\mathbf{k}_n.(\mathbf{r}-\tau\mathbf{u}_c) + \omega_{on}\tau\right]\right\} \end{aligned}$$

where Greek subscripts are not summed. This result shows that the turbulent field is convected by the mean flow and the peak of the cross correlation function decreases with the time τ of separation. The turbulent velocity field exhibits a convective feature and a time-dependence with this type of modelling.

References

[1]Tam, C.K.W., 1995, Computational aeroacoustics: issues and methods, *AIAA Journal*, **33**(10), 1788-1796.

[2]Lele, S.K., 1997, Computational Aeroacoustics: a review, *35th Aerospace Sciences Meeting & Exhibit*, AIAA Paper 97-0018.

[3]Bogey, C., Bailly, C. & Juvé, D., 1999, Computation of mixing layer noise using large eddy simulation, *5th AIAA/CEAS AeroAcoustics Conference*, AIAA Paper 99-1871.

[4]Mankbadi, R.R., Hixon, R., Shih, S.H. & Povinelli, L.A., 1998, Use of linearized Euler equations for supersonic jet noise prediction, *AIAA Journal*, **36**(2), 140-147.

[5]MORRIS, P.J., LONG, L.N., SCHEIDEGGER, T.E., WAND, Q. & PILON, A.R., 1998, High speed jet noise simulations, AIAA Paper 98-2290.

[6]KHAVARAN, A., KREJSA, E.A. & KIM, C.M., 1994, Computation of supersonic jet mixing noise for an axisymmetric convergent-divergent nozzle, *Journal of Aircraft*, **31**(3), 603-609.

[7]BÉCHARA, W., LAFON, P., BAILLY, C. & CANDEL, S., 1995, Application of a $k-\epsilon$ model to the prediction of noise for simple and coaxial free jets, *J. Acoust. Soc. Am.*, **97**(6), 3518-3531.

[8]BAILLY, C., LAFON, P. & CANDEL, S., 1996, Prediction of supersonic jet noise from a statistical acoustic model and a compressible turbulence closure, *J. Sound Vib.*, **194**(2), 219-242.

[9]BAILLY, C., LAFON, P. & CANDEL, S., 1997, Subsonic and supersonic jet noise predictions from statistical source models, *AIAA Journal*, **35**(11), 1688-1696.

[10]BÉCHARA, W., BAILLY, C., LAFON, P. & CANDEL, S., 1994, Stochastic approach to noise modeling for free turbulent flows, *AIAA Journal*, **32**(3), 455-463.

[11]BAILLY, C., LAFON, P. & CANDEL, S., 1995, A stochastic approach to compute noise generation and radiation of free turbulent flows, AIAA Paper 95-092.

[12]BAILLY, C., LAFON, P. & CANDEL, S., 1996, Computation of noise generation and propagation for free and confined turbulent flows, AIAA Paper 96-1732.

[13]LONGATTE, E., LAFON, P. & CANDEL, S., 1998, Computation of noise generation in internal flows, *4th AIAA/CEAS Aeroacoustics Conference*, AIAA Paper 98-2332.

[14]BOGEY, C., BAILLY, C. & JUVÉ, D., 1999, CAA approaches applied to mixing layer noise computation using LES, *EAA / ASA Forum Acusticum*, 14-19 March, Berlin.

[15]KRAICHNAN, R.H., 1970, Diffusion by a random velocity field, *Phys. Fluids*, **13**(1), 22-31.

[16]KARWEIT, M., BLANC-BENON, P., JUVÉ, D. & COMTE-BELLOT, G., 1991, Simulation of the propagation of an acoustic wave through a turbulent velocity field: A study of phase variance, *J. Acoust. Soc. Am.*, **89**(1), 52-62.

[17]DRUMMOND, I.T., DUANE, S. & HORGAN, R.R., 1984, Scalar diffusion in simulated helical turbulence with molecular diffusivity, *J. Fluid Mech.*, **138**, 75-91.

[18]DRUMMOND, I.T. & MÜNCH, W., 1990, Turbulent stretching of line and surface elements, *J. Fluid Mech.*, **215**, 45-59.

[19]TAM, C.K.W. & WEBB, J.C., 1993, Dispersion-relation-preserving finite difference schemes for computational acoustics, *J. Comput. Phys.*, **107**, 262-281.

[20]HU, F.Q., HUSSAINI, M.Y. & MANTHEY, J.L., 1996, Low-dissipation and low-dispersion Runge-Kutta schemes for computational acoustics, *J. Comput. Phys.*, **124**, 177-191.

[21]TAM, C.K.W., AURIAULT, L. & CAMBULI, F., 1998, Perfectly matched layer as an absorbing boundary condition for the linearized Euler equations in open and ducted domains, *J. Comput. Phys.*, **144**, 213-234.

[22]BAILLY, C. & JUVÉ, D., 1998, Numerical solution of acoustic propagation problems using linearized's Euler equations, AIAA Paper 98-2267, accepted in the AIAA Journal.

[23]GRÈVERIE, L. & BAILLY, C., 1998, Construction d'un opérateur de propagation à partir des équations d'Euler linéarisées, *C. R. Acad. Sci. Paris*, IIb, **326**(11), 741-746.

[24]LUSH, P.A., 1971, Measurements of subsonic jet noise and comparison with theory, *J. Fluid Mech.*, **46**(3), 477-500.

[25]VON KÁRMÁN, T., 1948, Progress in the statistical theory of turbulence, *Journal of Marine Research*, **7**, 252-264.

[26]PAO, Y.H., 1965, Structure of turbulent velocity and scalar fields at large wave numbers, *The Physics of Fluids*, **8**(6), 1063-1075.